THEORETICAL ANALYSIS OF V(Z) CURVES MEASURED BY ACOUSTIC LINE-FOCUS BEAM

J. Kushibiki, A. Ohkubo, and N. Chubachi

Faculty of Engineering
Tohoku University
Sendai, Japan

Abstract

This paper describes a theoretical analysis of the V(z) curves obtained by the nonscanning reflection acoustic microscope system using a line-focus beam. The analysis has been applied numerically to calculate a V(z) curve for a ZY-sapphire and compared with the experimental results at a frequency of 179 MHz using an acoustic sapphire line-focus-beam lens with a cylindrical concave surface of 1.0 mm radius. According to the analysis, it is shown that the shape and the periodic intervals of dips appearing in the V(z) curves are determined dominantly by the propagation properties of leaky SAWs. Further, the effect of leaky SAW parameters, i.e., phase velocity and attenuation factor, on the variation of V(z) curves is numerically investigated with use of an idealized reflectance function where only propagation characteristics of leaky SAWs are taken into account to provide a general interpretation of the V(z) curve measurements. It is shown that the velocity of leaky SAW determines the interval of dips in V(z) curves, while the attenuation factor affects the shape of V(z) curves.

1. Introduction

Recently, the nonscanning reflection acoustic microscope system using a line-focus beam has been successfully introduced for characterizing solid materials, including acoustic anisotropy [1]-[5]. The material characterization is made by measurements of the propagation characteristics of leaky SAWs whose velocities are determined from the V(z) curve measurements. The V(z) curves are unique and characteristic of materials so that they play a very important role in the material characterization.

Analyses for the V(z) curves have been extensively made in order to interpret a contrast mechanism in acoustic images observed by the mechanically scanned acoustic microscope system [6] with a conventional conical beam and the numerical V(z) curves have been also calculated to explain the experimental curves for some typical materials [7]-[9]. The calculations have been made in three-dimensional space, but some approximations should be made for the numerical analysis because of the complexity of calculations, and they have also a disadvantage that it is difficult to calculate properly the V(z) curves for anisotropy materials. On the other hand, the V(z) curves for a line-focus beam are analyzed in two-dimensional space because the line-focus beam is linearly focused along one axis with the structure of the cylindrical wavefront [10], so that the analysis has some advantages that there are less approximations and the anisotropy of solid materials can be reasonably taken into consideration in calculations.

In this paper, the V(z) curves obtained by the acoustic line-focus beam are theoretically analyzed and compared with the experimental results for a sapphire sample at a frequency of 179 MHz using an acoustic sapphire line-focus-beam lens with a cylindrical concave surface of 1.0 mm radius. Further, on the base of the analysis developed here, the effect of leaky SAW parameters, i.e., phase velocity and attenuation factor, on the variation of V(z) curves is numerically investigated with use of an idealized reflectance function where only propagation characteristics of leaky SAWs are taken into account to provide a general interpretation of the V(z) curve measurements.

2. Theoretical Analysis

To get the theoretical representation of V(z) curves, let us consider the cross-section geometry as shown in Fig. 1 for analyzing V(z) curves obtained by the acoustic line-focus-beam lens. The V(z) curves (for example, see Fig. 5) are the records of the piezoelectric transducer output as a function of distance between the acoustic probe and a sample, when the sample is moved along the z axis. Analysis is made in two-dimensional x-z plane by assuming that the acoustic fields do not vary in the y direction from the fact that the acoustic focused fields have a phase structure of cylindrical wavefront. In Fig. 1, an acoustic line-focus-beam lens has the following lens parameters: ℓ; the distance between a transducer and the top surface of the lens, R; the radius of curvature, and θ_M; the half-aperture angle, and a is the halfwidth of transducer. Co-ordinates x_0, x_1, x_2 and x_3 are placed on the transducer, the acoustic lens, the focal and the sample planes, respectively. For the simple description of the analysis, x_1 is on the acoustic lens plane.

0090-5607/82/0000-0623 $00.75 © 1982 IEEE

Acoustic waves radiated from the transducer at x_0 propagate into a sapphire rod and are linearly focused along the y axis and converted into a line-focus beam by an acoustic lens placed at x_1 with a cylindrical concave surface. The line-focus beam illuminates the sample at x_3 with traveling a distance z from the focal point. The reflected waves are collected again by the same lens, and then the acoustic fields are detected by the transducer. Here at each position of x_0, x_1, x_2 and x_3 we describe the acoustic fields for the forward-traveling waves as $u_0^+(x_0)$, $u_1^+(x_1)$, $u_2^+(x_2)$ and $u_3^+(x_3)$, where the superscript + means the 'forward', and the backward-traveling waves can be also designated by the superscript - for the corresponding fields.

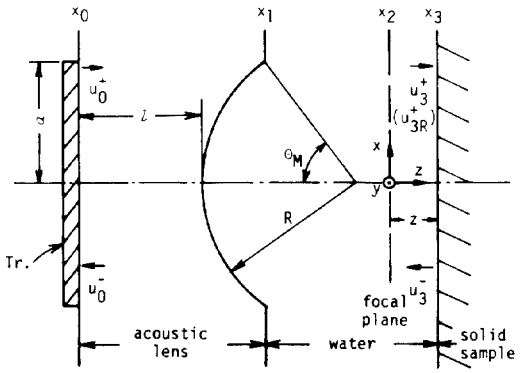

Fig. 1. Cross-section geometry of acoustic line-focus-beam lens and coordinate system used for analysis.

The analysis is carried out according to a theory[8],[9] based on Fourier optics. The transformations between the position x in planes parallel to the sample surface and the spatial frequency k_x which means the x component of the wavenumber k_l in the coupling liquid of water are given as follows:

$$U(k_x) = F\{u(x)\} = \int_{-\infty}^{\infty} u(x)\exp(-jk_x x)dx, \quad (1)$$

and

$$u(x) = F^{-1}\{U(k_x)\} = \int_{-\infty}^{\infty} U(k_x)\exp(jk_x x)dk_x, \quad (2)$$

where F and F^{-1} denote the Fourier transform and the inverse Fourier transform, respectively.

Taking the reflectance function $R(k_x)$ for a sample which reflects the elastic information of the solid sample at the water/sample interface, the relation between the incident field $U_3^+(k_x)$ and the reflected field $U_3^-(k_x)$ at the sample plane is expressed as

$$U_3^-(k_x) = R(k_x)U_3^+(k_x). \quad (3)$$

Therefore,

$$u_3^-(x_3) = F^{-1}\{R(k_x)U_3^+(k_x)\}, \quad (4)$$

and the field $U_3^+(k_x)$ are related to the field $U_2^+(k_x)$ at the focal plane as follows:

$$U_3^+(k_x) = U_2^+(k_x)\exp(jk_z z), \quad (5)$$

and then

$$u_3^+(x_3) = F^{-1}\{F\{u_2^+(x_2)\}\exp(jk_z z)\}, \quad (6)$$

where k_z is the z component of the wavenumber k_l defined as

$$k_z = (k_l^2 - k_x^2)^{1/2}. \quad (7)$$

The output voltage V(z) of the piezoelectric transducer is a function of the distance z because $u_0^-(x_0)$ varies with z and is represented as follows:

$$V(z) = A\int_{-\infty}^{\infty} u_0^+(x_0)u_0^-(x_0)dx_0. \quad (8)$$

where A is the arbitrary constant. Equation (8) can be rewritten by using the Rayleigh-Sommerfeld diffraction formula[11] for sound propagation and the Fourier analysis as follows:

$$V(z) = A\int_{-\infty}^{\infty} u_{3R}^+(x_3)u_3^-(x_3)dx_3, \quad (9)$$

where $u_{3R}^+(x_3)$ is the reference field defined as

$$u_{3R}^+(x_3) = \frac{T^-(x_1)}{T^+(x_1)}u_3^+(x_3). \quad (10)$$

The quantities $T^+(x_1)$ and $T^-(x_1)$ are the transfer coefficients from acoustic lens to water and from water to lens, respectively. They include the effect of acoustic antireflection coating layer with a quarter-wavelength thickness for reducing the transmission loss due to the large acoustic discontinuity at the sapphire-lens/water interface. The fields $u_3^+(x_3)$ and $u_3^-(x_3)$ have been already given in Eqs. (6) and (4), respectively.

Thus, the transducer output of V(z) obtained with the acoustic line-focus beam is represented by both the reference field $u_{3R}^+(x_3)$, determined uniquely by the employed acoustic line-focus-beam lens, and the reflected field $u_3^-(x_3)$, containing the acoustic response $R(k_x)$ of the sample which strongly depends on the wave propagation direction when the sample is anisotropic about the z axis.

3. Numerical Calculation and Discussion

3.1. V(z) curve for ZY-sapphire

According to the theoretical analysis of the transducer output V(z) in the acoustic microscope developed in the previous section, as an example, numerical calculations are carried out for a ZY-sapphire where leaky SAWs propagate in the Y direction on the interface of water/Z-cut-sapphire. For comparing the numerical results with the experimen-

tal results, we have chosen the following lens parameters: curvature radius; R=1.0 mm, half-aperture angle; θ_M=60°, distance; ℓ=12.0 mm, and acoustic frequency; f=179 MHz. The physical constants of each material required for the calculations are the same as Ref. 1.

Figure 2 shows the calculated spatial frequency spectrum distribution of acoustic fields of the line-focus beam at the focal plane as a function of normalized spatial frequency k_x/k_ℓ, where the effect of acoustic antireflection coating layer is taken into consideration. This beam has normalized spatial frequency spectra of being distributed to about 0.8. This can be easily seen from the fact that the half-aperture angle is limited to be 60° which corresponds to a normalized spatial frequency of 0.86.

Figure 3 shows the calculated reflectance function $R(k_x)$ for the water/ZY-sapphire interface as a function of normalized spatial frequency, where the solid and broken lines are for the phase and amplitude of $R(k_x)$, respectively. As seen in the figure, the phase has a distinct feature of turning by 180° at the critical angle $\theta_{\ell saw}$ for a leaky SAW, while the amplitude is unity in the region of the critical angle for a longitudinal wave and over the critical angle for a shear wave. The phase reversal is the most meaningful factor which is closely associated with the dip interval appearing in V(z) curves.

Figure 4 shows the numerically calculated V(z) curve for ZY-sapphire by employing the results of the acoustic fields in Fig. 2 and the reflectance function in Fig. 3. An experimental V(z) curve observed with a transducer of 1.55x1.55 mm^2 is shown in Fig. 5 for comparison. It can be seen that the experimental V(z) curve is, as a whole, explained well in the shape and the dip interval of the V(z) curve agrees well for the both V(z) curves. The dip intervals Δz relating to the measurement of the leaky SAW velocity $v_{\ell saw}$ are given in Table 1 with the values of $v_{\ell saw}$ calculated by the following equation[12],[13]:

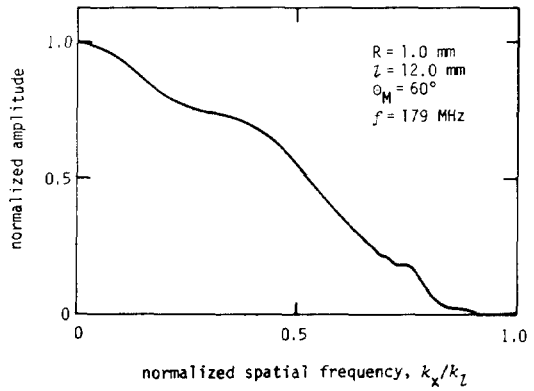

Fig. 2. Spatial frequency spectrum distribution of acoustic fields formed by a line-focus-beam lens at the focal plane.

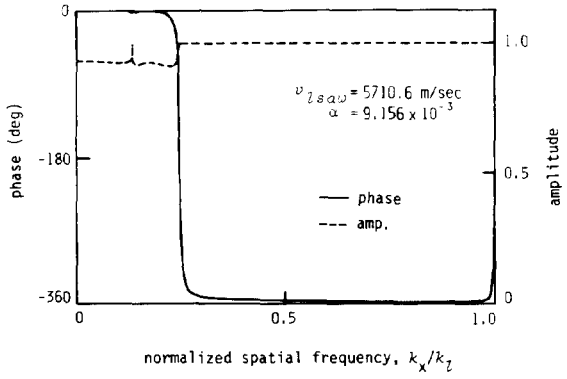

Fig. 3. Reflectance function for water/ZY-sapphire boundary.

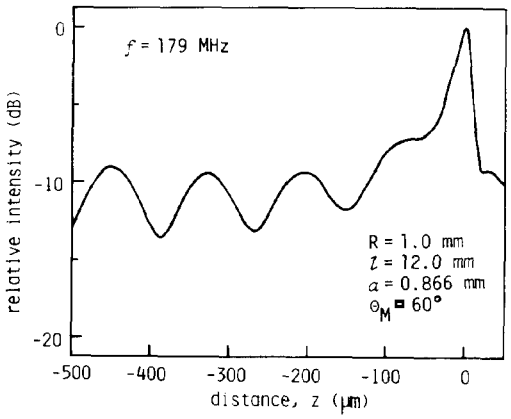

Fig. 4. V(z) curve numerically calculated for ZY-sapphire with acoustic line-focus beam at 179 MHz.

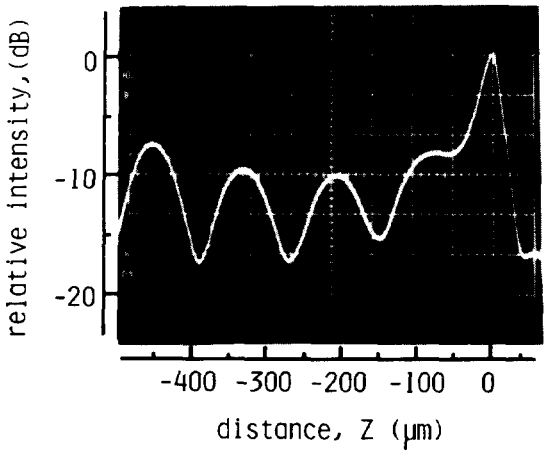

Fig. 5. V(z) curve experimentally measured for ZY-sapphire with acoustic line-focus beam at 179 MHz.

$$v_{lsaw} = v_l/(1-(1-v_l/2f\Delta z)^2)^{1/2}, \quad (11)$$

where v_l is the longitudinal velocity in water. The values of Δz and v_{lsaw} obtained by the present analysis for the V(z) curve are in good agreement with the values obtained experimentally. Both the velocity values of leaky SAWs also agree well with the theoretical velocity value[1] obtained by the exact numerical calculation of leaky SAWs propagating on the water/ZY-sapphire boundary.

3.2. Effect of leaky SAW parameters on V(z) curves

Now, let us discuss the effect of the leaky SAW parameters, that is, phase velocity and attenuation factor, on the variation of V(z) curves in order to give a general interpretation of the V(z) curve measurements.

For the purpose, an idealized reflectance function is introduced in calculations where only propagation characteristics of leaky SAWs are taken into account. The idealized reflectance function $R(k_x)$ is given as follows:

$$R(k_x) = \frac{k_x - k^*_{lsaw}}{k_x - k_{lsaw}} . \quad (12)$$

The solution k_{lsaw} is defined by

$$k_{lsaw} = \frac{2\pi f}{v_{lsaw}}(1+j\alpha), \quad (13)$$

where v_{lsaw} and α are the phase velocity and the attenuation factor for leaky SAW, respectively. In this way we can examine separately how each of the two parameters v_{lsaw} and α affects the V(z) curves.

First let us consider the effect of leaky SAW velocity v_{lsaw} on V(z) curves when the normalized attenuation factor α is fixed to be constant.

Table 1. Comparison of theoretical and experimental results relating to velocity measurement for leaky SAWs obtained by V(z) curves on ZY-sapphire.

	Dip interval Δz (μm)	Laeky SAW velocity v_{lsaw} (m/s)
Numerical analysis	119.0	5670
Experiment	120.3	5700
Exact analysis	——	5711

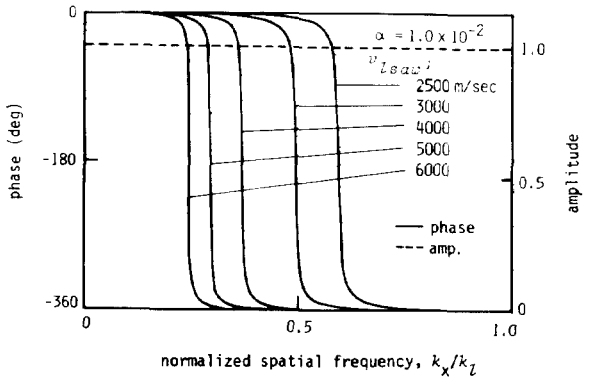

Fig. 6. Idealized reflectance function as a parameter of leaky SAW velocity with normalized attenuation factor of 1.0×10^{-2}.

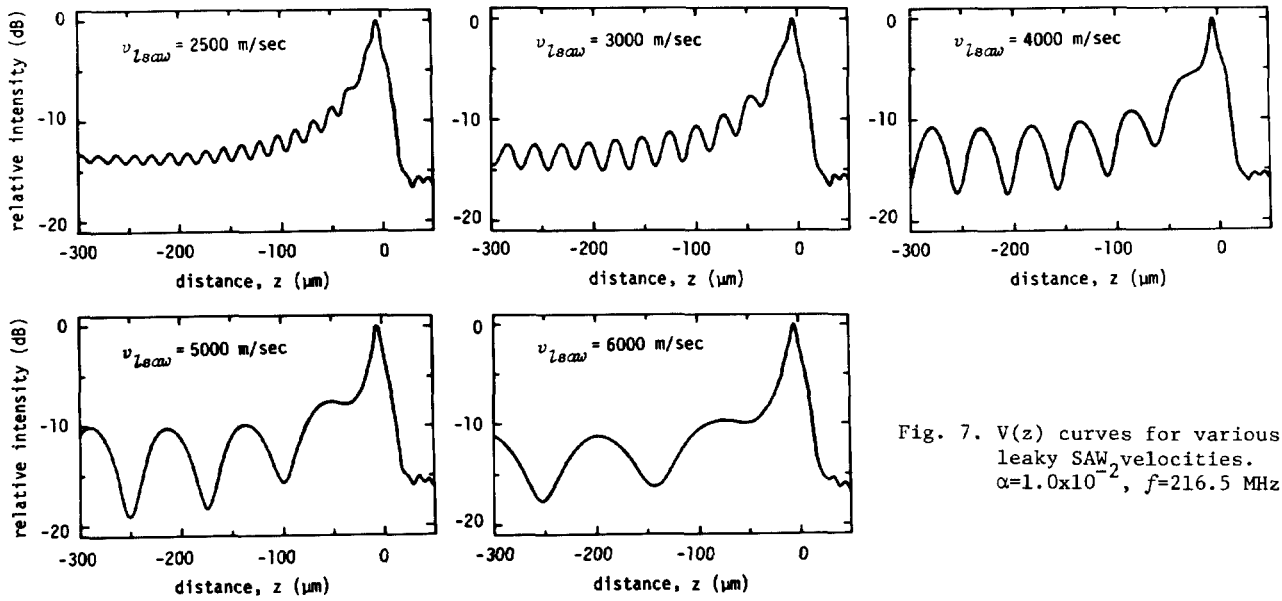

Fig. 7. V(z) curves for various leaky SAW velocities. $\alpha=1.0\times10^{-2}$, f=216.5 MHz.

Figure 6 shows the idealized reflectance functions as a parameter of leaky SAW velocity. As easily seen from the figure, the value of leaky SAW velocities is closely related to the spatial frequency giving rise to reversal in phase in the reflectance functions. Figure 7 shows the corresponding V(z) curves. For all cases, periodic variation appears in the negative region. As the velocity increases, the dip interval Δz obtained in the calculated V(z) curves becomes larger. The relationship between v_{lsaw} and Δz obtained by the numerical calculations is coincident with Eq. (11). As for the depth of dips in the V(z) curves, there can be seen a tendency to decrease the depth as the leaky SAW velocity decreases. This is caused by the fact that the acoustic field distribution incident on the sample surface has less amplitude for the spatial frequency component required for exciting leaky SAW with slow velocity on the water/sample interface.

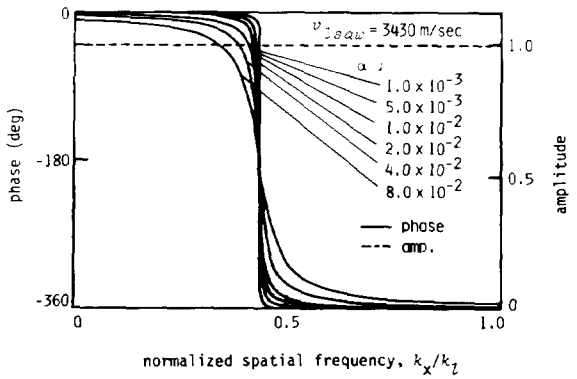

Fig. 8. Idealized reflectance functions as a parameter of normalized attenuation factor with leaky SAW velocity of 3430 m/s.

Next let us consider the effect of the normalized attenuation factor α on V(z) curves at a constant phase velocity of leaky SAW v_{lsaw}. Figure 8 shows the reflectance functions as a parameter of normalized attenuation factor in a case of v_{lsaw} = 3430 m/s, which corresponds to that for the water/fused-quartz interface. The value of a parameter α affects the gradient in the variation of phase around the critical angle in the reflectance functions. Figure 9 shows the corresponding V(z) curves. In the region of the attenuation factor 1.0×10^{-2} to 2.0×10^{-2}, the V(z) curves appear in a shape with deep and successive dips. In the region of a relatively smaller attenuation factor, shallow dips are seen still in succession. But in the region of smaller attenuation factor than 1.0×10^{-3}, it is difficult to obtain clear dips in V(z) curves. In the region of relatively larger attenuation factor 4.0×10^{-2}, the deep dips appear near the focal point and the amplitude of interference attenuates rapidly with decreasing of distance z. Furthermore, it is interesting to find that there is a peak with a larger amplitude than the amplitude at the focal point for the range of larger attenuation factor than about 8.0×10^{-2}. Thus the attenuation factor α remarkably affects the amplitude in interference patterns with the dip interval unvaried. This is attributed to the fact that the attenuation factor relates directly to the efficiency of exciting leaky SAWs on the sample surface or reradiating bulk waves into water.

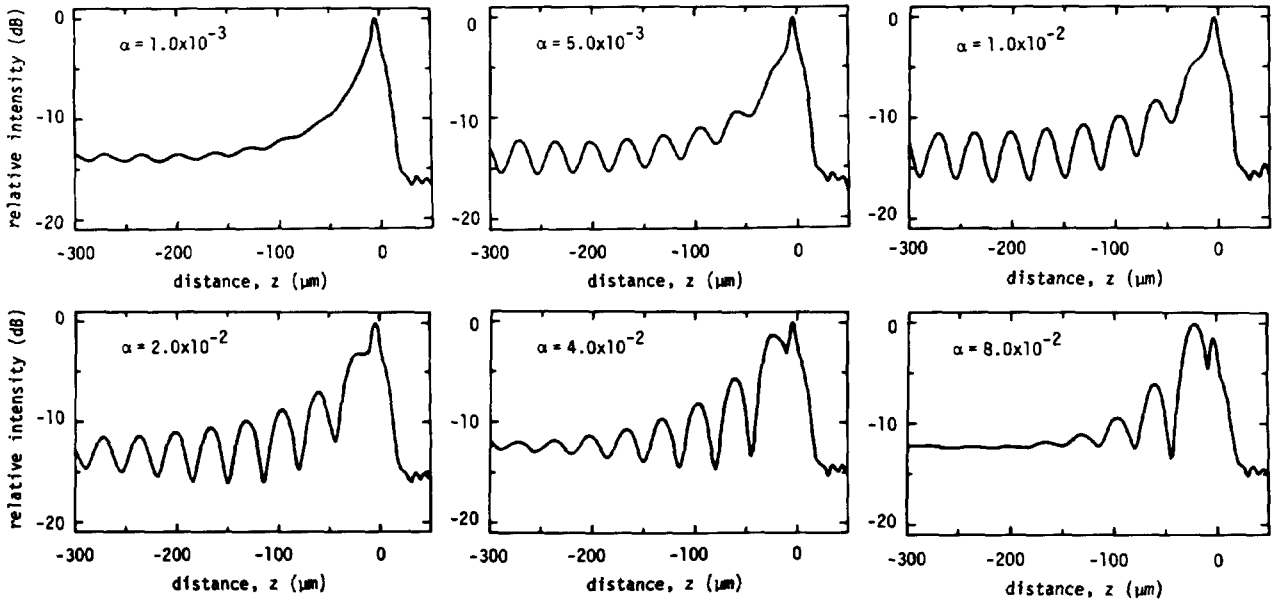

Fig. 9. V(z) curves for various normalized attenuation factors. v_{lsaw}=3430 m/s, f=216.5 MHz.

4. Conclusion

The theoretical analysis for the V(z) curves measured by a nonscanning reflection acoustic microscope system with a line-focus beam has been developed by using Fourier optics. The analyzed formula has been applied to numerically calculate the V(z) curve for the interface of water/ZY-sapphire and compared to the experimental V(z) curve at a frequency of 179 MHz using an acoustic sapphire line-focus-beam lens with a cylindrical concave surface of 1.0 mm radius. From the comparison, it has been confirmed that the V(z) curve numerically calculated for the ZY-sapphire sample agrees well with the experimental V(z) curve in both the shape and the dip interval. These results support theoretically that the nonscanning reflection acoustic microscope system with the line-focus beam can be appropriately applied to make measurements of leaky SAW velocities by using the relation (11) between the dip interval in V(z) curves and the leaky SAW velocity.

Furthermore, to show a general interpretation of the V(z) curve measurements, we have numerically investigated, according to the analysis, the effect of leaky SAW parameters, i.e., phase velocity and attenuation factor, on the variation of V(z) curves with the introduction of an idealized reflectance function where only propagation characteristics of leaky SAWs are taken into account. It has been shown that the velocity of leaky SAW determines the interval of dips in V(z) curves, while the attenuation factor affects the shape of V(z) curves.

Acknowledgements

The authors are very grateful to K. Horii and H. Maehara for their helpful discussions and experimental assistance. This work was supported in part by the Grant-in-Aids for Scientific Research from the Ministry of Education, Science & Culture, Japan.

References

1 J.Kushibiki, A.Ohkubo, and N.Chubachi:'Anisotropy detection in sapphire by acoustic microscope using line-focus beam', Electron. Lett., **17**, pp.534-536 (1981).
2 J.Kushibiki, A.Ohkubo, and N.Chubachi:'Acoustic anisotropy detection of materials by acoustic microscope using line-focus beam', IEEE Ultrasonics Symp. Proc., pp.552-556 (1981).
3 J.Kushibiki, A.Ohkubo, and N.Chubachi:'Propagation characteristics of leaky SAWs on water/$LiNbO_3$ boundary measured by acoustic microscope with line-focus beam', Electron. Lett., **18**, pp.6-7 (1982).
4 J.Kushibiki, K.Horii, and N.Chubachi:'Leaky SAW velocity on water/silicon boundary measured by acoustic line-focus beam', Electron. Lett., **18**, pp.732-734 (1982).
5 J.Kushibiki, A.Ohkubo, and N.Chubachi:'Material characterization by acoustic microscope with line-focus beam', 12th Acoustical Imaging Symp. Proc., (in press).
6 C.F.Quate, A.Atalar, and H.K.Wickramasinghe: 'Acoustic microscopy with mechanical scanning — A review', Proc. IEEE, **67**, pp.1092-1114 (1979).
7 A.Atalar, C.F.Quate, and H.K.Wickramasinghe: 'Phase imaging in reflection with the acoustic microscope', Appl. Phys. Lett., **31**, pp.791-793 (1977).
8 A.Atalar:'An angular-spectrum approach to contrast in reflection acoustic microscope', J. Appl. Phys., **49**, pp.5130-5139 (1978).
9 H.K.Wickramasinghe:'Contrast in reflection acoustic microscopy', Electron. Lett., **14**, pp.305-306 (1978).
10 J.Kushibiki, A.Ohkubo, and N.Chubachi:'Linearly focused acoustic beams for acoustic microscopy', Electron. Lett., **17**, pp.520-522 (1981).
11 J.W.Goodman:'Introduction to Fourier optics' (McGraw-Hill, New York, 1968), Chap. 2.
12 W.Parmon and H.L.Bertoni:'Ray interpretation of the material signature in the acoustic microscope', Electron. Lett., **15**, pp.684-686 (1979).
13 A.Atalar:'A physical model for acoustic signatures', J. Appl. Phys., **50**, pp.8237-8239 (1979).